

Spin excitations of the correlated semiconductor FeSi probed by THz radiation

V. V. Glushkov,^{1,*} B. P. Gorshunov,^{1,†} E. S. Zhukova,^{1,†} S. V. Demishev,^{1,†}
A. A. Pronin,¹ N. E. Sluchanko,¹ S. Kaiser,² and M. Dressel²

¹*A. M. Prokhorov General Physics Institute of RAS, 38, Vavilov str., Moscow, 119991, Russia*

²*1. Physikalisches Institut, Universität Stuttgart, Pfaffenwaldring 57, 70550 Stuttgart, Germany*

(Dated: February 5, 2022)

By direct measurements of the complex optical conductivity $\sigma(\nu)$ of FeSi we have discovered a broad absorption peak centered at frequency $\nu_0(4.2 \text{ K}) \approx 32 \text{ cm}^{-1}$ that develops at temperatures below 20 K. This feature is caused by spin-polaronic states formed in the middle of the gap in the electronic density of states. We observe the spin excitations between the electronic levels split by the exchange field of $H_e = 34 \pm 6 \text{ T}$. Spin fluctuations are identified as the main factor determining the formation of the spin polarons and the rich magnetic phase diagram of FeSi.

The origin of the narrow gap ($E_g \sim 60 \text{ meV}$) that develops in the density of electronic states of FeSi at low temperatures poses a real challenge to both theorists and experimentalists for last five decades [1, 2]. Due to the anomalous transfer of spectral weight from the gap region to high energies (up to $10E_g$) [3–5] FeSi was put in line with the Kondo insulators $\text{Ce}_3\text{Bi}_4\text{Pt}_3$, SmB_6 , YbB_{12} *etc.* At the same time, the crossover from an activated to a Curie-Weiss behavior of the magnetic susceptibility [6] was successfully explained within a spin-fluctuation model suggesting thermally induced magnetic moments of Fe [7]. Finally, the distinct d -symmetry of electronic states above and below the gap [8] makes it important to consider carefully the effects of strong electron correlations [9–12].

The interest to FeSi has been renewed after recent high resolution photoemission experiments, which show no sign of a Kondo resonance favoring a simple itinerant semiconductor picture with d -bands renormalized due to correlation effects [13, 14]. Ellipsometric studies in a broad spectral range supports this assumption [15]; the collapse of the gap is caused by a temperature-induced transition from a low-temperature semiconductor to a high-temperature semimetal. However, this conclusion is at variance with the results of dc-transport and magnetic studies [16–18] which assign the onset of the metallic state below 80 K to the formation of a narrow many-body resonance (width $E_p \sim 6 \text{ meV}$) within the gap. The tiny but finite residual intensity at the Fermi level was also found in low-energy photoemission spectra [19]. Hence, it is particularly important to identify the intra-gap features that are responsible for the anomalous ground state properties of FeSi and to compare them with the prediction of existing theories [9–12, 20].

In this Letter we report on the first direct measurements of the complex optical conductivity $\sigma(\nu) = \sigma_1 + i\sigma_2$ of FeSi in the low-frequency range $8 - 40 \text{ cm}^{-1}$, supplemented by broad-range experiments in an unprecedented large spectral range from 10 Hz to $1.2 \times 10^{15} \text{ Hz}$. We identify a spin-polaronic resonance in the middle of the energy gap that is split by the exchange field $H_e = 34 \pm 6 \text{ T}$.

Excitations between these electronic levels lead to an anomalous contribution to $\sigma(\nu)$ around $\nu_0 = 32 \text{ cm}^{-1}$. From the comparison between the intra-gap excitation parameters of FeSi, SmB_6 and YbB_{12} [21–23] we conclude that the low-temperature optical properties of these compounds cannot be accounted for within the Kondo insulator model.

Single crystals of FeSi under investigation were grown by Czochralski technique. The samples were cut and subsequently polished by abrasive diamond powder. The fragility of the crystals constituted a limit of how thin the samples could be polished (about 35 to 50 μm). In order to remove the surface defects induced by polishing, the specimens were etched in the mixture of hydrofluoric, nitric and acetic acids taken at the ratio of 2:3:2. Note, σ_{dc} of polished crystals exceeds that of etched samples by more than two orders of magnitude (Fig. 2), we limited our optical studies to thoroughly etched samples.

A quasioptical THz spectrometer based on backward wave oscillators [21] was employed to measure the transmission and phase spectra in the spectral range from 8 to 40 cm^{-1} at temperatures $4 \text{ K} < T < 20 \text{ K}$. From these quantities the complex optical conductivity is calculated. Additional infrared reflection measurements were conducted with a Bruker IFS 113V ($50 - 10^4 \text{ cm}^{-1}$) complemented by a spectrometric ellipsometer (Woolam VASE, up to $4 \times 10^4 \text{ cm}^{-1}$). The microwave conductivity was measured by cavity-perturbation technique at fixed frequencies 9.5, 35 and 100 GHz using Gunn diodes as radiation sources. Radiofrequency investigations (10 – 1000 MHz) were carried out utilizing a HP Impedance Analyzer HP4191A. Standard four-probe technique was applied to obtain $\sigma_{\text{dc}}(T)$ used as reference data at zero frequency. The Kramers-Kronig analysis of the infrared reflectivity spectra was performed by utilizing the directly measured values of σ_1 and σ_2 below and above the infrared range. Eventually we obtained a very wide panorama of the optical conductivity $\sigma_1(\nu)$ and of the dielectric function $\epsilon_1(\nu) = 1 - 4\pi\sigma_2(\nu)/\nu$.

Figure 1 presents the spectra of $\sigma_1(\nu)$ and $\epsilon_1(\nu)$ directly calculated [21] from the frequency dependent

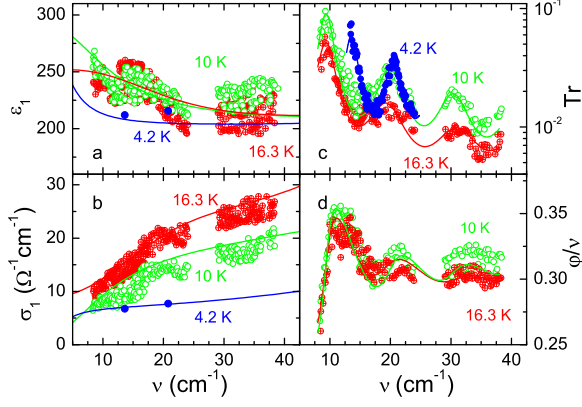


FIG. 1: (Color online) Terahertz spectra of (a) optical conductivity σ_1 and (b) dielectric function ϵ_1 of FeSi calculated from (c) transmission Tr and (d) normalized phase shift φ/ν at $T = 4.2$ K, 10 K and 16.3 K (blue, green, and red symbols, respectively). Solid lines present the results of the least-square fitting by Eq.1 (a,b) or by interferometric equations (c,d). The error bars for the 4.2 K data in panels a,b are within the symbols.

transmission $Tr(\nu)$ (panel c) and phase shift $\varphi(\nu)/\nu$ (panel d). Due to the large refractive index of $n = (\epsilon_1)^{1/2} \approx 14.5 - 15.8$ and relatively low absorption the interference within these very thin samples causes well resolved fringes. The dispersion of the ac-conductivity in the terahertz range from 17 to 40 cm^{-1} [Fig. 1(b)] is small

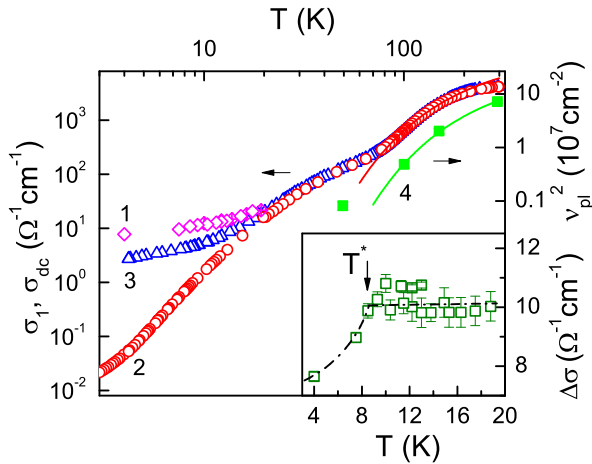


FIG. 2: (Color online) Terahertz conductivity $\sigma_1(T)$ of FeSi measured at $\nu=21$ cm^{-1} (1) in comparison with the static conductivity $\sigma_{dc}(T)$ of etched (2) and polished (3) samples. Activation asymptotics of σ_{dc} and the squared plasma frequency ν_{pl}^2 (4) $\sigma_{dc}, \nu_{pl}^2 \propto \exp(-E_g/2k_B T)$ are shown by solid lines. Inset presents the difference $\Delta\sigma(T) = \sigma_1(T) - \sigma_{dc}(T)$. Arrow points to a kink on $\Delta\sigma(T)$ at $T^* \sim 8$ K.

compared to that caused by the tails of optical conductivity expected from interband transitions or infrared optical phonons [24]. The optical conductivity decreases even further when T falls below 20 K [Fig. 1(b)]. The comparison of $\sigma_1(T)$ with the dc data is plotted in Fig. 2. At low temperatures the terahertz conductivity saturates at a rather high value of approximately 10 $(\Omega\text{cm})^{-1}$; about two orders of magnitude above the dc conductivity. Note the rather large difference between the dc conductivity of etched and polished sample (curves 2 and 3 in Fig. 2). It demonstrates that surface defects can mask the intrinsic properties of FeSi in optical, transport and photoemission studies.

An essential information about low-energy electro-dynamics of FeSi can be extracted from the wide-range spectra of $\sigma_1(\nu)$ and $\epsilon_1(\nu)$ plotted in Fig. 3. The evolution of $\sigma_1(\nu)$ shows that the Drude contribution becomes gradually weaker as the temperature is lowered; below 100 K no Drude roll-off can be resolved in the gap any more. Correspondingly the low-frequency dielectric constant becomes positive at $T < 100$ K; this provides evidence that the compound enters an insulating state at

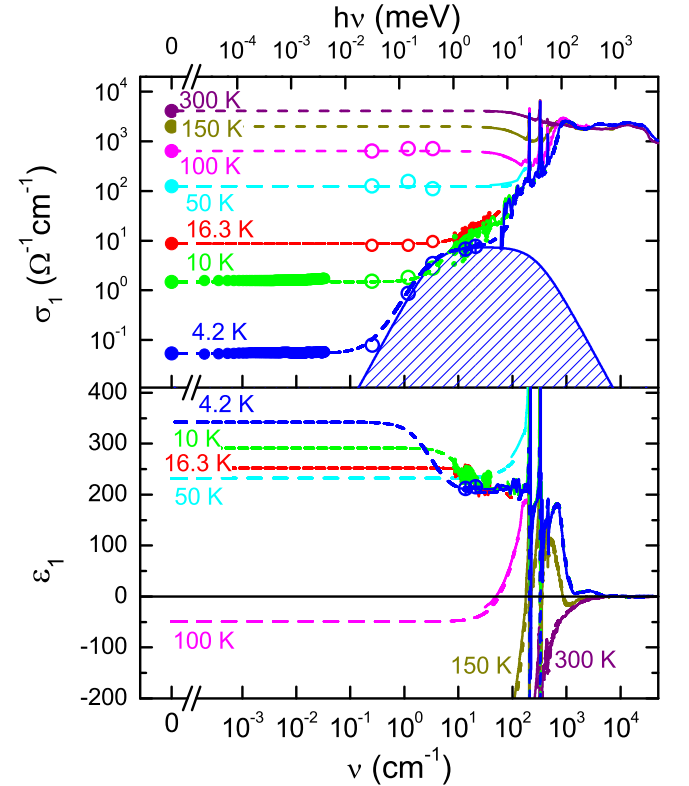


FIG. 3: (Color online) Wide range optical conductivity σ_1 and dielectric function ϵ_1 of FeSi at temperatures 4.2 – 300 K. Dashed lines represent the results of least-square fitting by Eq. (1). The σ_{dc} values are shown by filled circles at zero frequency in upper panel. Shaded area shows the terahertz resonance contribution at $T = 4.2$ K with the parameters given in Tab. I.

low temperature. Most important for the present Communication, when T drops below 20 K $\sigma_1(\nu)$ exhibits a wide step-like feature between 0.1 and 10 cm^{-1} that is accompanied by a corresponding step in $\epsilon(\nu)$.

Applying the scaling relations [24] $(\sigma_1\nu)^2 \propto (h\nu - E_{\text{dir}})$ and $(\sigma_1\nu)^{0.5} \propto (h\nu \pm E_{\text{ph}} - E_{\text{ind}})$ (here E_{ph} is the characteristic phonon energy), we obtain the direct and indirect energy gaps at $T=4.2$ K as depicted in Fig.4. The value of $E_{\text{dir}} \approx 650 \text{ cm}^{-1}$ (corresponding to 81 meV) confirms previous reports [3, 15]. However, combining $E_{\text{ind}} - E_{\text{ph}} \approx 44 \text{ cm}^{-1}$ (5.5 meV) with $E_{\text{ind}} + E_{\text{ph}} \approx 410 \text{ cm}^{-1}$ (51 meV) results in a rather low value of $E_{\text{ind}} \approx 227 \text{ cm}^{-1}$ (28.4 meV), which is only half of the energy gap $E_g = 60 \text{ meV}$ reported previously based on transport measurements [3, 16, 18] (Fig.2). Note also that the obtained characteristic phonon frequency $E_{\text{ph}} = 183 \text{ cm}^{-1}$ agrees very well the E mode (180 cm^{-1}) that shows the largest broadening with increasing temperature due to strong electron-phonon interaction [25].

In order to clarify the discrepancy between transport gap ($E_g \approx 60 \text{ meV}$) and indirect optical gap ($E_{\text{ind}} \sim 30 \text{ meV}$) we fit the conductivity and dielectric data, $\sigma_1(\nu)$ and $\epsilon_1(\nu)$, by the sum of Drude and Lorentz terms [26]:

$$\sigma(\nu) = \frac{\nu_{\text{pl}}^2}{\gamma_0 - i\nu} + \frac{1}{2} \sum_{i=1}^N \frac{\Delta\epsilon_i \nu_{0i}^2 \nu}{\gamma_i \nu + i(\nu_{0i}^2 - \nu^2)} \quad (1)$$

where ν_{pl} , and γ_0 are plasma frequency and scattering rate of charge carriers, ν_{0i} , $\Delta\epsilon_i$, and γ_i are eigenfrequency, dielectric contribution and damping (for i th Lorentzian), respectively. The fits are shown by dashed lines in Fig. 3. The number of Lorentz contributions N was chosen minimal to describe the dispersion due to optical phonons and interband transitions; the estimated parameters of the features agree well with previous attempts [3, 15]. The Drude contribution to the fit yields a plasma frequency ν_{pl} that follows the activation law $\nu_{\text{pl}}^2 \propto \exp\{-E_g/2k_B T\}$ with $E_g \sim 70 \text{ meV}$ for $T > 100 \text{ K}$ (Fig. 2). This observation proves that charge carriers are thermally excited from the lower to the upper band. The energy gap E_g of FeSi eventually becomes irrelevant but its size does not change with increasing temperature. Along these lines, the lower value of $E_{\text{ind}} \sim 30 \text{ meV}$ corresponds to a finite density of states inside the gap rather than to a shift of bands. This suggestion is supported by the broad absorption identified in the terahertz conductivity for $T < 20 \text{ K}$ (Fig. 3). Comparing the Lorentzian parameters listed in Tab. I we see that $\Delta\epsilon$ and γ increase with lowering temperature while ν_0 stays approximately constant ($\nu_0 = 4 \pm 0.5 \text{ meV}$). Note that the enormous increase of the damping from $\gamma \approx 3.7 \text{ meV}$ to 35 meV when the temperature is reduced from 16 to 4.2 K rules out the assignment of this broad feature to excitations from extrinsic defects or impurity band.

In order to obtain a better insight into the origin of the anomalous terahertz contribution to the optical re-

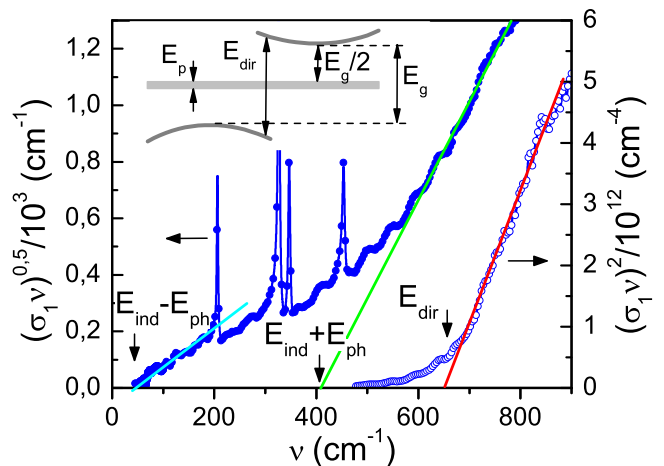


FIG. 4: (Color online) The scaling of $\sigma_1(\nu, T = 4.2 \text{ K})$ data by the relations $(\sigma_1\nu)^2 \propto (h\nu - E_{\text{dir}})$ and $(\sigma_1\nu)^{0.5} \propto (h\nu \pm E_{\text{ph}} - E_{\text{ind}})$ allows for determination of the direct and indirect gaps (see text) [24]. Solid lines correspond to the least-squares fits. The proposed band structure of FeSi is sketched in the inset.

sponse, let us consider the excess conductivity $\Delta\sigma(T) = \sigma_1(T) - \sigma_{\text{dc}}(T)$ plotted in the inset of Fig. 2. At temperatures $8 \text{ K} < T < 20 \text{ K}$ $\Delta\sigma(T) = 10 \pm 1 \text{ } (\Omega\text{cm})^{-1}$ is approximately constant; but below $T^* \approx 8 \text{ K}$ it drops rapidly down to $\Delta\sigma(4.2 \text{ K}) \approx 7.5 \text{ } (\Omega\text{cm})^{-1}$. It is important to note that the value of T^* is very close to the “freezing” temperature of interacting quasiparticles $T_m \approx 7 \text{ K}$ found previously from transport and magnetic studies [27]. These quasiparticles (i.e. spin polarons) correspond to the states of the many-body resonance (of width $E_p \sim 6 \text{ meV}$), which appears at the Fermi level below 80 K due to on-site Hubbard repulsion [16]. This now explains the smaller value of the indirect gap $E_{\text{ind}} \approx E_g/2$ that defines the position of this resonance in the middle of the energy gap (see inset in Fig. 4).

We can conclude that in FeSi due to strong on-site Coulomb repulsion below $T \approx 80 \text{ K}$ a many-body resonance appears in the electronic density of states right in the middle of the energy gap [16]. The exchange field of $H_e \approx 34 \pm 6 \text{ T}$ splits the band, and spin excitations between the resultant electronic levels cause the anomalous terahertz contribution to the optical conductivity of FeSi. The inherent resonance width $E_g \approx 6 \text{ meV}$ corresponds

TABLE I: The parameters of Lorentz terms used to fit the terahertz absorption feature in $\sigma(\nu)$ of FeSi at different temperatures T . $\Delta\epsilon = (\nu_{\text{pl}}/\nu_0)^2$ describes the oscillator strength, ν_0 the center frequency, and γ the damping parameter.

T (K)	$\Delta\epsilon$	ν_0 (cm^{-1})	γ (cm^{-1})
4.2	107 ± 30	32 ± 5	280 ± 30
10	94 ± 10	36 ± 10	280 ± 40
16.3	28 ± 5	25 ± 5	30 ± 10

to the binding energy of spin polaronic states [16] The extremely large damping $\gamma \approx 280 \text{ cm}^{-1}$ ($\approx 35 \text{ meV}$) is an estimate of the spin-fluctuation rate.

This approach allows us to interpret the terahertz feature in the $\sigma_1(\nu)$ spectra: since the energy of the mode is extremely low ($h\nu_0 \ll E_{\text{ind}}$), we probe excitation within the intra-gap many-body resonance. Using the oscillator strength $\Delta\epsilon\nu_0^2 = (1.1 \pm 0.4) \times 10^5 \text{ cm}^{-2}$ (Tab. I) and effective mass $m^* \approx m_0$, we can estimate the particles concentration $n_0 = \pi m^* \Delta\epsilon\nu_0^2 / e^2 = (1.2 \pm 0.4) \times 10^{18} \text{ cm}^{-3}$ that contribute to the terahertz absorption at $T = 4.2 \text{ K}$. The remarkable agreement of n_0 with the effective concentration of the many-body states $n_{\text{sp}} \approx 10^{17} - 10^{18} \text{ cm}^{-3}$ [16, 27] strongly supports a spin-polaronic ground state of FeSi. The terahertz absorption can then be associated with intra-gap excitations between the electronic levels split by the exchange field $H_e = h\nu_0 / (2\mu_B) = 34 \pm 6 \text{ T}$, which agrees well with the value of $H_e = 35 \pm 10 \text{ T}$ previously estimated from magnetic studies [17]. The very large damping $\gamma \approx 35 \text{ meV}$ at low temperatures indicates strong spin fluctuations that cause transitions between the excited spin states and the ground state with a relaxation time $\tau = (2\pi c\gamma)^{-1} \approx 1.9 \times 10^{-14} \text{ s}$. Both, the low concentration n_0 and the large damping γ below 10 K make it difficult to detect this feature in photoemission experiments [14, 19].

Furthermore, our finding gives us now the possibility to distinguish also between different types of intra-gap excitations observed in the far infrared spectra of other strongly correlated electron systems identified as Kondo insulators [1, 2]. Similar features have been observed in the $\sigma(\nu)$ spectra of SmB₆ [21, 22] and YbB₁₂ [23] and are ascribed to exciton-polaronic states that appear in the gap due to $4f - 5d$ charge fluctuations. The parameters of the Lorentz terms extracted for SmB₆ ($\nu_0 \approx 24 \text{ cm}^{-1}$, $\Delta\epsilon \approx 12$ and $\gamma \approx 7 \text{ cm}^{-1}$ [21, 22]) and YbB₁₂ ($\nu_0 \approx 22 \text{ cm}^{-1}$, $\Delta\epsilon \approx 75$ and $\gamma \approx 15 \text{ cm}^{-1}$ [23]) characterize the exciton-polaronic complexes that arise from the coupling of itinerant electrons to soft valence fluctuations [28]. The characteristic times of charge fluctuations ($\tau \propto \gamma^{-1} \approx (4 - 8) \times 10^{-13} \text{ s}$ for SmB₆ and YbB₁₂) and spin fluctuations ($\tau \propto 1.9 \times 10^{-14} \text{ s}$ for FeSi) are significantly different because of the different origin of the ground states. Further theoretical treatments are required to thoroughly understand this novel aspect of strongly correlated electron systems.

The authors are grateful to Prof. A.A.Menovsky for the grown FeSi single crystals. This work was supported by RAS Programme “Strongly Correlated Electrons” and Federal Programme “Scientific and Educational Human Resources of Innovative Russia”.

* Electronic address: glushkov@lt.gpi.ru; Also at: Moscow Institute of Physics and Technology, 9 Institutskii per., Dolgoprudnyi, Moscow Region 141700 Russia

† Also at: Moscow Institute of Physics and Technology, 9 Institutskii per., Dolgoprudnyi, Moscow Region 141700 Russia

- [1] J. Aeppli and Z. Fisk, Comments Condens. Matter Phys., **16**, 155 (1992).
- [2] P. S. Riseborough, Adv. Phys., **49**, 257 (2000).
- [3] Z. Schlesinger, Z. Fisk, H.-T. Zhang, M. B. Maple, J. DiTusa, and G. Aeppli, Phys. Rev. Lett., **71**, 1748 (1993).
- [4] L. Degiorgi, M. B. Hunt, H. R. Ott, M. Dressel, B. J. Fenstra, G. Grüner, Z. Fisk, and P. Canfield, Europhys. Lett., **28**, 341 (1994).
- [5] F. P. Mena, J. F. DiTusa, D. van der Marel, G. Aeppli, D. P. Young, A. Damascelli, and J. A. Mydosh, Phys. Rev. B, **73**, 085205 (2006).
- [6] V. Jaccarino, G. K. Wertheim, J. H. Wernick, L. R. Walker, and S. Arajs, Phys. Rev., **160**, 476 (1967).
- [7] I. Takahashi, Journal of Physics: Condensed Matter, **9**, 2593 (1997).
- [8] C. Fu and S. Doniach, Phys. Rev. B, **51**, 17439 (1995).
- [9] V. I. Anisimov, S. Y. Ezhov, I. S. Elfimov, I. V. Solov'yev, and T. M. Rice, Phys. Rev. Lett., **76**, 1735 (1996).
- [10] V. V. Mazurenko, A. O. Shorikov, A. V. Lukoyanov, K. Kharlov, E. Gorelov, A. I. Lichtenstein, and V. I. Anisimov, Phys. Rev. B, **81**, 125131 (2010).
- [11] M. Figueira and R. Franco, Eur. Phys. J. B, **58**, 1 (2007).
- [12] R. Franco, J. Silva-Valencia, and M. Figueira, Eur. Phys. J. B, **67**, 159 (2009).
- [13] D. Zur, D. Menzel, I. Jursic, J. Schoenes, L. Patthey, M. Neef, K. Doll, and G. Zwirgagl, Phys. Rev. B, **75**, 165103 (2007).
- [14] M. Klein, D. Zur, D. Menzel, J. Schoenes, K. Doll, J. Röder, and F. Reinert, Phys. Rev. Lett., **101**, 046406 (2008).
- [15] D. Menzel, P. Popovich, N. N. Kovaleva, J. Schoenes, K. Doll, and A. V. Boris, Phys. Rev. B, **79**, 165111 (2009).
- [16] N. E. Sluchanko, V. V. Glushkov, S. V. Demishev, M. V. Kondrin, K. M. Petukhov, N. A. Samarin, V. V. Moshchalkov, and A. A. Menovsky, EPL (Europhysics Letters), **51**, 557 (2000).
- [17] N. E. Sluchanko, V. V. Glushkov, S. V. Demishev, A. A. Menovsky, L. Weckhuysen, and V. V. Moshchalkov, Phys. Rev. B, **65**, 064404 (2002).
- [18] M. Corti, S. Aldrovandi, M. Fanciulli, and F. Tabak, Phys. Rev. B, **67**, 172408 (2003).
- [19] M. Arita, K. Shimada, Y. Takeda, M. Nakatake, H. Namatame, M. Taniguchi, H. Negishi, T. Oguchi, T. Saitoh, A. Fujimori, and T. Kanomata, Phys. Rev. B, **77**, 205117 (2008).
- [20] T. Jarlborg, Phys. Rev. B, **76**, 205105 (2007).
- [21] B. Gorshunov, N. Sluchanko, A. Volkov, M. Dressel, G. Knebel, A. Loidl, and S. Kunii, Phys. Rev. B, **59**, 1808 (1999).
- [22] N. E. Sluchanko, V. V. Glushkov, B. P. Gorshunov, S. V. Demishev, M. V. Kondrin, A. A. Pronin, A. A. Volkov, A. K. Savchenko, G. Grüner, Y. Bruynseraede, V. V. Moshchalkov, and S. Kunii, Phys. Rev. B, **61**, 9906 (2000).

- [23] B. Gorshunov, P. Haas, O. Ushakov, M. Dressel, and F. Iga, Phys. Rev. B, **73**, 045207 (2006).
- [24] P. Y. Yu and M. Cardona, *Fundamentals of Semiconductors* (Springer, 2010).
- [25] A.-M. Racu, D. Menzel, J. Schoenes, and K. Doll, Phys. Rev. B, **76**, 115103 (2007).
- [26] M. Dressel and G. Grüner, *Electrodynamics of Solids* (Cambridge University Press, 2002).
- [27] V. V. Glushkov, I. Voskoboinikov, S. V. Demishev, I. Krivitskii, A. A. Menovsky, V. V. Moshchalkov, N. Samarin, and N. E. Sluchanko, JETP, **99**, 394 (2004).
- [28] K. A. Kikoin and A. S. Mishchenko, J. Phys.: Condens. Matter, **7**, 307 (1995).